Journal of Power Sources 184 (2008) 557–561

Contents lists available at ScienceDirect

Journal of Power Sources

journal homepage: www.elsevier.com/locate/jpowsour

Short communication

Pillared layered $Li_{1-2x}Ca_xCoO_2$ cathode materials obtained by cationic exchange under hydrothermal conditions

Zhanxu Yang, Wensheng Yang*, Zhanfeng Tang

State Key Laboratory of Chemical Resource Engineering, Beijing University of Chemical Technology, Beijing 100029, China

ARTICLE INFO

Article history:
Received 4 December 2007
Received in revised form 16 February 2008
Accepted 18 February 2008
Available online 10 March 2008

Keywords:
Lithium battery
Cathode material
Pillared layered $Li_{1-2x}Ca_xCoO_2$
Cationic exchange
Hydrothermal synthesis

ABSTRACT

A simple method has been employed to prepare pillared layered $Li_{1-2x}Ca_xCoO_2$ cathode materials by cationic exchange under hydrothermal conditions. The synthesized materials were characterized by means of X-ray diffraction (XRD), inductively coupled plasma-atomic emission spectroscopy (ICP-AES), field emission scanning electron microscope (FE-SEM) and galvanostatic charge–discharge cycling. The XRD data of the products show that they are single phases and retain the layered α-$NaFeO_2$ type structure. The FE-SEM images of the materials prepared by hydrothermal method show uniform small particles, and the particle size of the materials is about 200 nm. The initial discharge specific capacities of layered $LiCoO_2$ and pillared layered $Li_{0.946}Ca_{0.027}CoO_2$ cathode materials calcined at 800 °C for 5 h within the potential range of 3.0–4.3 V (vs. Li^+/Li) are 144.6 and 142.3 mAh g^{-1}, respectively, and both materials retain good charge–discharge cycling performance. However, with increasing upper cutoff voltage, the pillar effect of Ca^{2+} in $Li_{1-2x}Ca_xCoO_2$ becomes more significant. The pillared layered $Li_{0.946}Ca_{0.027}CoO_2$ has a higher capacity with an initial discharge specific capacity of 177.9 and 215.8 mAh g^{-1} within the potential range of 3.0–4.5 and 4.7 V (vs. Li^+/Li), respectively, and retains good charge–discharge cycling performance.

1. Introduction

α-$NaFeO_2$ type layered $LiCoO_2$ (space group $R\bar{3}m$) has been the dominant cathode material for commercial Li-ion batteries since 1991 because of its ease of production, high operating voltage, low self-discharge rate and high reversibility. In this structure, LiO_6 and CoO_6 octahedra share their corners and stack alternatively along the *c*-axis direction, which allows two-dimensional diffusion of Li ions during electrochemical deintercalation and intercalation processes [1].

However, the specific capacity of $LiCoO_2$ is relatively low at around 140 mAh g^{-1} because only about 0.5 Li per $LiCoO_2$ can be reversibly cycled without causing serious capacity loss [2]. To obtain a higher capacity from $LiCoO_2$, it must be charged above 4.3 V (vs. Li^+/Li) to use more than 0.5 Li per $LiCoO_2$ [3]. However, charge–discharge cycling using a higher upper cutoff voltage often results in a rapid capacity loss, thought to be caused by side reactions with electrolyte at high potentials and the structure instability that the removal of the lithium ions during extraction results in a set of phase changes, i.e. from O3 → H1–3 → O1 and the O3 → H1–3 phase change near 4.5 V leading to rapid capacity loss in Li_xCoO_2 [2–7]. To overcome this problem, many works have been reported to improve the structure stability of $LiCoO_2$ by coated some materials on its particles or doped other metals into the structure [3,5,7]. However, the capacity retention of coated or doped $LiCoO_2$ is still unacceptable for practical applications. Our laboratory has reported that pillared layered $Li_{1-2x}Ca_xCoO_2$ synthesized by a molten salt ion exchange method can suppress the unwanted phase transition because Ca^{2+} ions in the interlayer galleries prevent local collapse of the interslab space and act as pillars during the deintercalation process [8]. However, this method has a complicated process which limits the industrial application.

Recently, hydrothermal synthesis [9–11] is reported to prepare layered $LiCoO_2$ cathode material in that this method is a useful route for preparing uniform small particles and also has other advantages such as a simple process and low synthesis temperature.

In this work, a much more simple method is firstly employed to synthesize pillared layered $Li_{1-2x}Ca_xCoO_2$ cathode materials by cationic exchange reactions between Li^+, Ca^{2+} and H^+ of CoOOH under hydrothermal conditions. The structures, the morphologies and the electrochemical behaviors of pillared layered $Li_{1-2x}Ca_xCoO_2$ have been discussed in detail.

* Corresponding author. Tel.: +86 10 6443 5271; fax: +86 10 6442 5385.
E-mail address: yangws@mail.buct.edu.cn (W. Yang).

0378-7753/$ – see front matter © 2008 Elsevier B.V. All rights reserved.
doi:10.1016/j.jpowsour.2008.02.034

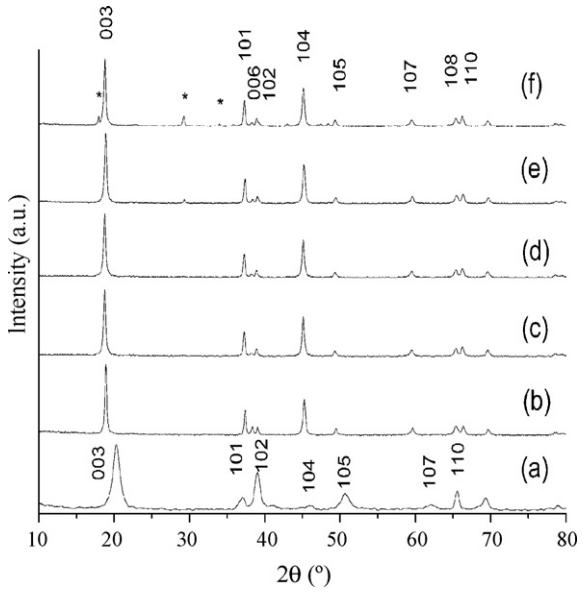

Fig. 1. XRD patterns of the CoOOH precursor (a) and products from different initial Ca/Co molar ratios of (b) 0, (c) 0.05, (d) 0.1, (e) 0.3 and (f) 0.5. Reflections from $Ca(OH)_2$ are indicated with*.

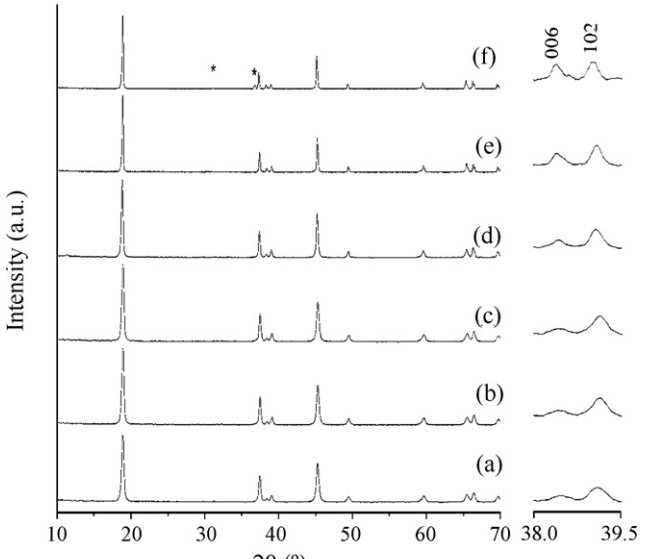

Fig. 2. XRD patterns of $Li_{0.946}Ca_{0.027}CoO_2$ calcined at (a) 400, (b) 500, (c) 600, (d) 700, (e) 800 and (f) 900 °C in air for 5 h. Reflections from Co_3O_4 are indicated with *. Right small figure is the local area enlargement of (0 0 6) and (1 0 2) peaks from 38.0 to 39.5°.

2. Experimental

2.1. Synthesis of materials

Layered $LiCoO_2$ and pillared layered $Li_{1-2x}Ca_xCoO_2$ cathode materials were prepared by cationic exchange reactions between Li^+ (and Ca^{2+}) and H^+ of CoOOH under hydrothermal conditions. CoOOH was initially prepared by oxidation of $Co(OH)_2$ which was made by adding a 2 mol L^{-1} NaOH solution dropwise to a 0.5 mol L^{-1} $CoSO_4$ $7H_2O$ solution (200 mL). The addition of NaOH solution was terminated when the pH value of the solution reached about 12 and subsequently was treated by adding a quantity of 30% H_2O_2 solution. CoOOH was stirred in 80 mL of LiOH (or LiOH and $Ca(OH)_2$) aqueous solution, then the resulting suspension was

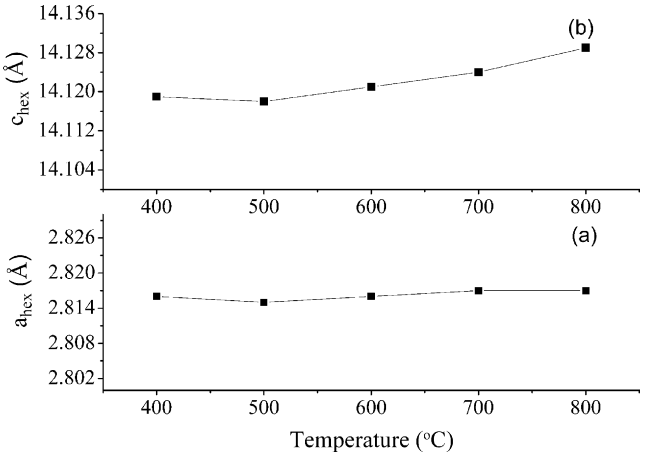

Fig. 3. Variations of a_{hex} and c_{hex} parameters of $Li_{0.946}Ca_{0.027}CoO_2$ calcined at different temperatures.

hydrothermally treated at 220 °C for 10 h in autoclave. After the reaction, the resulting precipitate was collected by filtration and then dried at 100 °C for 12 h to obtain $Li_{1-2x}Ca_xCoO_2$. In order to improve the crystallinity, the resulting $Li_{1-2x}Ca_xCoO_2$ was calcined at different temperatures in air.

2.2. Characterization of materials

The crystal structures of the products were analyzed by means of X-ray diffraction (XRD) (Shimadzu XRD-6000) that was operated at 40 kV and 30 mA from 10 to 80° at the wavelength of Cu Kα radiation (λ = 0.15406 nm). Elemental analyses for Li, Co and Ca were examined by inductively coupled plasma-atomic emission spectroscopy (ICP-AES) (Shimadzu ICPS-7500). The particle morphologies of the products were observed by means of field emission scanning electron microscope (FE-SEM) (Hitachi S-4700).

Electrochemical behaviors during charge–discharge cycles were examined using a two-electrode test cell with lithium foil as the negative electrode. A positive electrode was made by coating a paste of active material, acetylene black and polyvinylidene fluoride (PVDF) binder (80:10:10 wt.%) on an aluminum-foil collector. The positive film was subjected to roll press and the electrodes of 10 mm diameter (the mass of active material for each electrode is about 4 mg) were punched out. The positive electrodes were dried at 110 °C for 12 h in a vacuum oven. The coin-type cells (CR 2032) were assembled in an argon filled glove box with an electrolyte of 1 mol L^{-1} $LiPF_6$ in EC-EMC-DMC (1:1:1 volume ratio) solution and a separator of Celgard 2400. The electrochemical data were collected using LAND CT2001A test system within the potential range of 3.0–4.3, 4.5 or 4.7 V (vs. Li/Li^+) at a constant current density of 0.1 mA cm^{-2} (25 mA g^{-1}).

3. Results and discussion

The products were synthesized by mixing CoOOH precursor, $LiOH{\cdot}H_2O$ and $Ca(OH)_2$ with different initial Ca/Co molar ratios of 0, 0.05, 0.1, 0.3 and 0.5 under hydrothermal conditions. The XRD pattern of the CoOOH precursor shows the formation of a single phase as shown in Fig. 1a. Moreover, the structure of CoOOH (space group $R\bar{3}m$) is found to be similar to that of $LiCoO_2$. Therefore, $LiCoO_2$ can be prepared by cationic exchange reactions between Li^+ and H^+ of CoOOH under hydrothermal conditions [9,10]. The powder XRD patterns and the results of element analysis of samples prepared by cationic exchange under hydrothermal conditions at different initial Ca/Co molar ratios are shown in Fig. 1b–f and Table 1, respectively. The data of Table 1 show that the content of Li^+ in samples

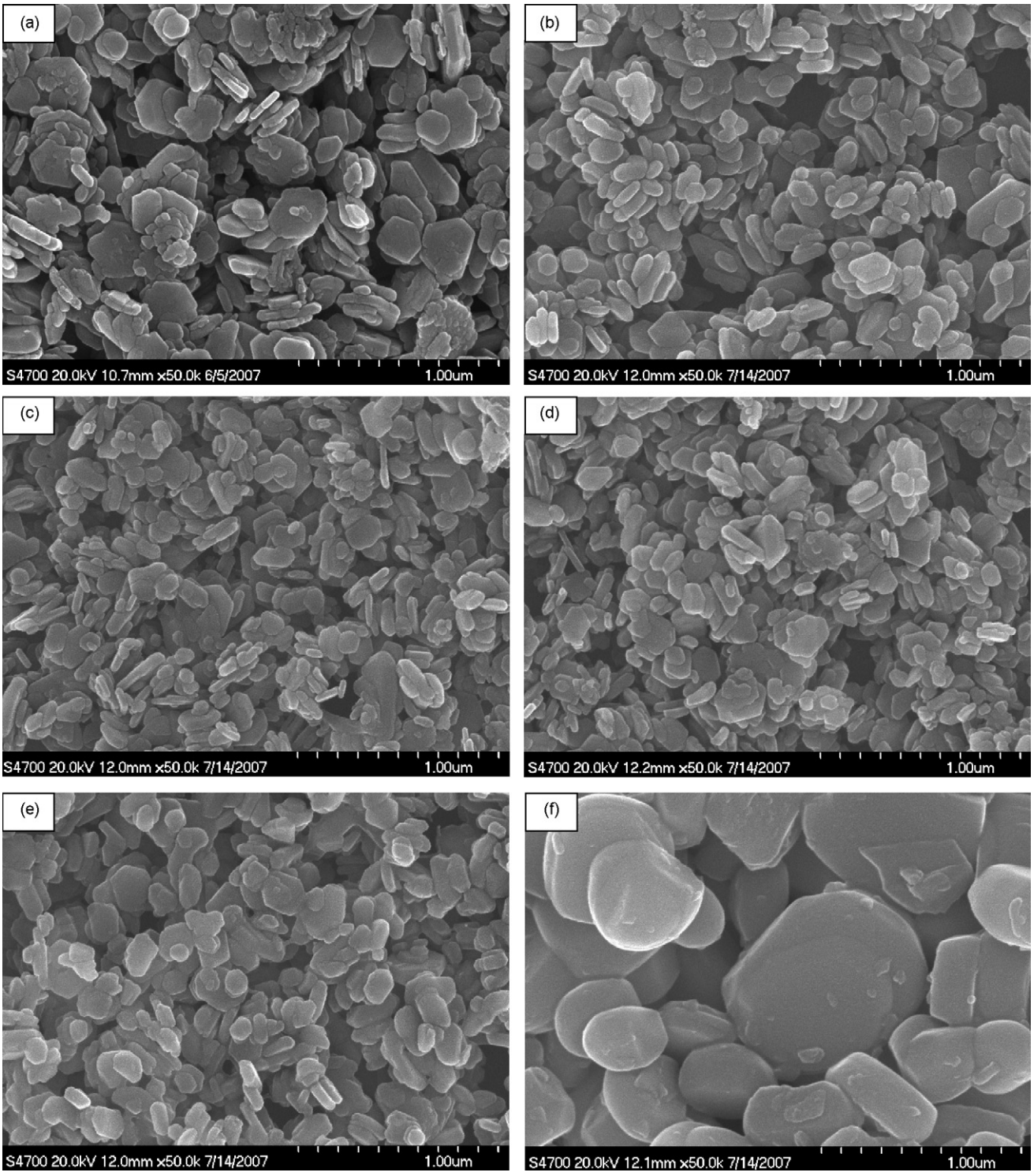

Fig. 4. FE-SEM micrographs of hydrothermally synthesized $Li_{0.946}Ca_{0.027}CoO_2$ (a) and products after calcination at (b) 400, (c) 500, (d) 600, (e) 700 and (f) 800 °C in air for 5 h.

decrease and the content of Ca^{2+} increase in relationship of 2:1 with the initial Ca/Co molar ratios of 0.05 and 0.1. In addition, the XRD patterns indicate that the products prepared at initial Ca/Co molar ratios of 0, 0.05 and 0.1 are single phases and retain the layered α-$NaFeO_2$ type structure. Sequentially increasing initial molar ratios of Ca/Co, the content of Li^+ still decrease, however, a small quantity of $Ca(OH)_2$ cannot be completely removed, which can also be proved by the results of XRD as shown in Fig. 1e–f. Therefore, we only choose the initial Ca/Co molar ratios of 0, 0.05 and 0.1 to do further research. The lattice parameters of the products from the initial Ca/Co molar ratios of 0, 0.05 and 0.1 are shown in Table 2. With different amounts of Ca^{2+} ions in the products, the *a*-axis value has little change, while the *c*-axis value increases obviously compared with that of $LiCoO_2$. Because the *a*-axis value is critically related to the metal–metal intraslab distance, and the *c*-axis value is related to the interslab distance between the CoO_2 sheets, these

Table 1
Molar percentages of elements Li and Ca (by regarding element Co as 100%) present in products obtained from different initial Ca/Co molar ratios

Initial Ca/Co molar ratio	Li (mol%)	Ca (mol%)	Ca/Li molar ratio of product
0	100.06	0.00	0
0.05	97.20	1.41	0.014/0.972
0.1	94.57	2.73	0.027/0.946
0.3	94.01	6.54	0.065/0.940
0.5	93.61	10.50	0.105/0.936

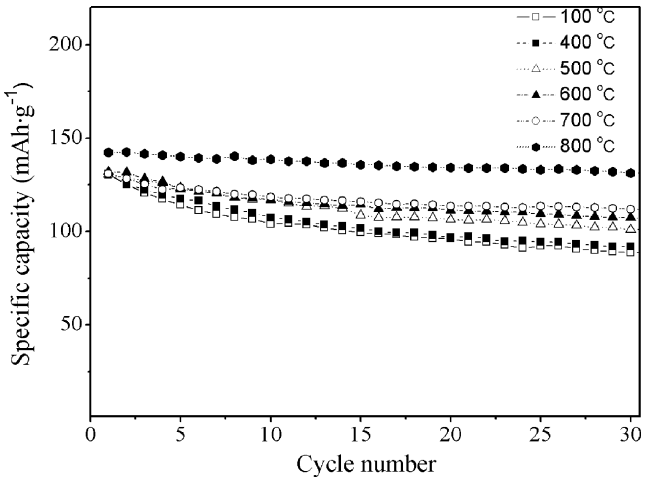

Fig. 5. Cycling performances of hydrothermally synthesized $Li_{0.946}Ca_{0.027}CoO_2$ cathode material calcined at different temperatures within the potential range of 3.0–4.3 V (vs. Li/Li^+) at a constant current density of 0.1 mA cm^{-2}.

results prove that Ca^{2+} ions in the products are situated in the interslab. The *c*-axis value of $Li_{1-2x}Ca_xCoO_2$ is larger than that of $LiCoO_2$ because the ionic radius of Ca^{2+} is larger than that of Li^+. A small amount of Ca^{2+} ions in the interslab space provides larger space for the movement of lithium ions, and can prevent the lattice from shrinking because of the unchangeable radius of Ca^{2+} during the deintercalation process. Liu et al. [12] and Pouillerie et al. [13,14] have also reported that Zn^{2+} or Mg^{2+} ions in the interstab space can prevent the local collapse of crystal due to pillar effect of Zn^{2+} or Mg^{2+} ions. Based on the above data from XRD and the research result of our laboratory [8], we choose the $Li_{0.946}Ca_{0.027}CoO_2$ material to do further research. Additionally, in order to further improve the crystallinity of electrode material which is critically related to specific capacity and cycling stability in Li-ion battery system, the hydrothermally synthesized $Li_{0.0946}Ca_{0.027}CoO_2$ material is calcined at different temperatures.

The XRD patterns of $Li_{0.946}Ca_{0.027}CoO_2$ calcined at 400, 500, 600, 700, 800 and 900 °C for 5 h in air are shown in Fig. 2. Lattice parameters of samples calculated by a least square method are shown in Fig. 3. With increasing the calcination temperature, the full width at the half-maximum becomes narrow which indicates the improvement of the crystallinity by the heat treatment, and separations of (0 0 6)/(1 0 2) peaks become much more distinct which indicates the formation of a highly ordered lamellar structure. However, when the calcination temperature increases to 900 °C, a small

Table 2
Lattice parameters of samples from different initial Ca/Co molar ratios prepared by cationic exchange under hydrothermal conditions

Initial Ca/Co molar ratio	Samples	*a* (Å)	*c* (Å)	V_{hex} (Å^3)
0	$LiCoO_2$	2.817	14.054	96.584
0.05	$Li_{0.972}Ca_{0.014}CoO_2$	2.817	14.110	96.689
0.1	$Li_{0.946}Ca_{0.027}CoO_2$	2.817	14.131	97.182

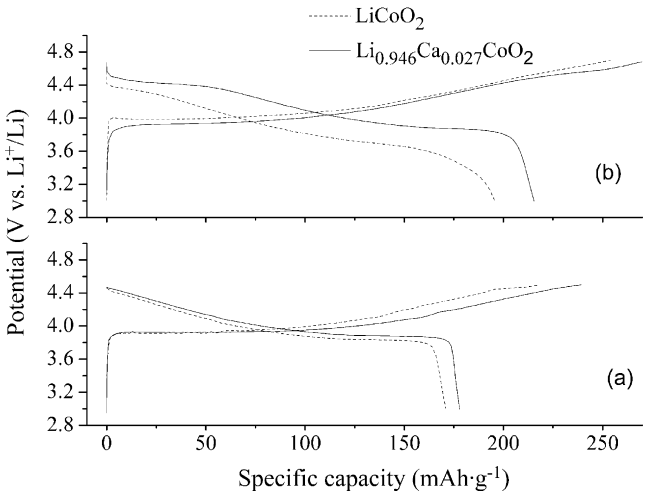

Fig. 6. Charge and discharge curves for hydrothermally synthesized $LiCoO_2$ and $Li_{0.946}Ca_{0.027}CoO_2$ calcined at 800 °C for 5 h within the potential range of 3.0–4.5 (a) and 3.0–4.7 V (b) (vs. Li/Li^+) at a constant current density of 0.1 mA cm^{-2}.

amount of spinel phase Co_3O_4 is found. Therefore, the calcination temperature should be chosen below 900 °C. Additionally, the calculated lattice constants *a* and *c* have little changes. These results indicate that Ca^{2+} ions are still localized in the interslab space during the calcination process.

The FE-SEM micrographs of hydrothermally synthesized $Li_{0.0946}Ca_{0.027}CoO_2$ and products after calcination at different temperatures are shown in Fig. 4. It is found that the hydrothermally synthesized material has uniform small particles and the particle size of products has no significant change after calcination between 400 and 700 °C. In addition, the images of products show similar shapes of the particles and the particle size is about 200 nm. However, when the calcination temperature increases to 800 °C, the particle size of the product has significant growth.

Fig. 5 shows the cycling behaviors of hydrothermally synthesized $Li_{0.946}Ca_{0.027}CoO_2$ cathode material calcined at different temperatures in the potential range of 3.0–4.3 V (vs. Li^+/Li) at a constant current density of 0.1 mA cm^{-2} (25 mA g^{-1}). The electrochemical cycling stabilities of all the samples after heat-treatment have been improved. The initial discharge specific capacity of the $Li_{0.946}Ca_{0.027}CoO_2$ product calcined at 800 °C for 5 h is 142.3 mAh g^{-1} and is much higher than that of other products. During subsequent cycles, the specific capacity decays slowly. A reversible capacity of 131.3 mAh g^{-1} is observed on the 30th cycle and is also much higher than that of other products. In comparison, the initial discharge specific capacity of $LiCoO_2$ cathode material which was synthesized by calcination at 800 °C for 5 h after hydrothermal reaction is 144.6 mAh g^{-1}, and this material has a discharge specific capacity of 124.2 mAh g^{-1} on the 30th cycle. Therefore, the pillared layered $Li_{0.946}Ca_{0.027}CoO_2$ shows less capacity fading than layered $LiCoO_2$.

From the above results, it is found that the product calcined at 800 °C exhibits the best cyclability with higher specific capacity, which can be mainly attributed to the improvement of crystallinity reflected by clear separations of (0 0 6)/(1 0 2) and (1 0 8)/(1 1 0) peaks as shown in Fig. 2. Furthermore, the heat treatment can make the Ca^{2+} ions more uniformly distributed in the interslab space, which may be another reason to improve the electrochemical performance of cathode material. In the further study, the upper cutoff voltage increases to 4.5 and 4.7 V (vs. Li^+/Li), and the corresponding first charge and discharge profiles of both layered $LiCoO_2$ and pillared layered $Li_{0.946}Ca_{0.027}CoO_2$ cathode material are given in Fig. 6. As shown in Fig. 6, the initial discharge specific capacity of pillared

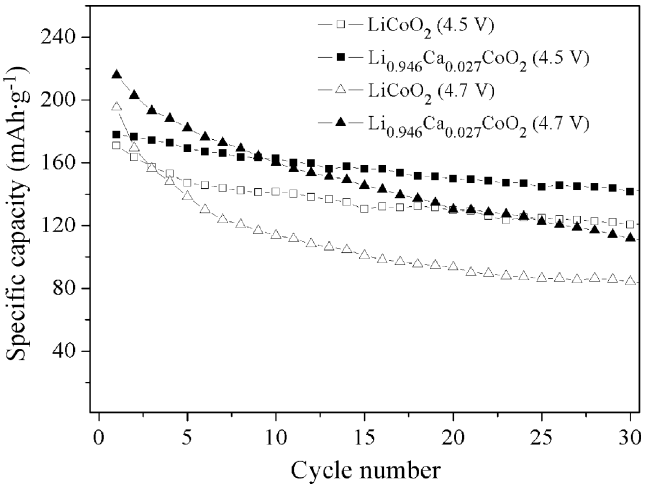

Fig. 7. Cycling performances of hydrothermally synthesized $LiCoO_2$ and $Li_{0.946}Ca_{0.027}CoO_2$ calcined at 800 °C for 5 h within the potential range of 3.0–4.5 and 4.7 V (vs. Li/Li^+) at a constant current density of 0.1 mA cm^{-2}.

layered $Li_{0.946}Ca_{0.027}CoO_2$ cathode material is 177.9 mAh g^{-1} in the potential range of 3.0–4.5 V and 215.8 mAh g^{-1} in the potential range of 3.0–4.7 V, and is much higher than that of layered $LiCoO_2$ material. Furthermore, the pillared layered $Li_{0.946}Ca_{0.027}CoO_2$ cathode material has lower charge plateau and higher discharge plateau which indicate higher lithium diffusion kinetics in the interslab space. Fig. 7 shows the variations in discharge specific capacity with cycle number of both products. It is evident that the $Li_{0.946}Ca_{0.027}CoO_2$ cathode material has a higher specific capacity and better capacity retention than $LiCoO_2$ under higher upper cut-off potential. These results can be attributable to the pillar effect of Ca^{2+} ions which provides larger space for the movement of lithium ions and prevents the local collapses of the structure during the lithium intercalation/deintercalation process.

4. Conclusions

A simple synthesis approach is successfully used to prepare pillared layered $Li_{1-2x}Ca_xCoO_2$ cathode materials with α-$NaFeO_2$ type single phase structure, and this method could be easily scaled up for industrial production. The layered pillared $Li_{1-2x}Ca_xCoO_2$ cathode materials prepared by this route have a higher specific capacity, a better overcharge tolerance and higher lithium diffusion coefficient than $LiCoO_2$. In addition, it is confirmed that a small amount of Ca^{2+} ions localized in the interslab space can significantly improve the electrochemical performance of the cathode material due to the pillar effect of Ca^{2+} ions which provides larger space for the movement of lithium ions and prevent the collapse of crystal during the lithium intercalation/deintercalation process.

Acknowledgments

This work was supported by the National Nature Science Foundation of China, the National 863 Plan (Grant No. 2006AA03Z343), the 111 Project (Grant No. B07004), and the Program for Changjiang Scholars and Innovative Research Team in University (Grant No. IRT0406).

References

[1] A.V.D. Ven, M.K. Aydinol, G. Ceder, J. Electrochem. Soc. 145 (1998) 2149–2155.
[2] T. Ohzuku, A. Ueda, J. Electrochem. Soc. 141 (1994) 2972–2977.
[3] Z. Chen, Z. Lu, J.R. Dahn, J. Electrochem. Soc. 149 (2002) A1604–A1609.
[4] Z. Chen, J.R. Dahn, Electrochim. Acta 49 (2004) 1079–1090.
[5] X. Sun, X.Q. Yang, J. McBreen, Y. Gao, M.V. Yakovleva, X.K. Xing, M.L. Daroux, J. Power Sources 97–98 (2001) 274–276.
[6] G.G. Amatucci, J.M. Tarascon, L.C. Klein, J. Electrochem. Soc. 143 (1996) 1114–1123.
[7] J.N. Reimers, J.R. Dahn, J. Electrochem. Soc. 139 (1992) 2091–2097.
[8] W.S. Yang, X.M. Li, L. Yang, D.G. Evans, X. Duan, J. Phys. Chem. Solids 67 (2006) 1343–1346.
[9] G.G. Amatucci, J.M. Tarascon, D. Larcher, L.C. Klein, Solid State Ionics 84 (1996) 169–180.
[10] Y.-M. Chiang, Y.-I. Jang, H. Wang, B. Huang, D.R. Sadoway, P. Ye, J. Electrochem. Soc. 145 (1998) 887–891.
[11] M. Okubo, E. Hosono, J. Kim, M. Enomoto, N. Lojima, T. Kudo, H. Zhou, I. Honma, J. Am. Chem. Soc. 129 (2007) 7444–7452.
[12] H. Liu, Q. Cao, L.J. Fu, C. Li, Y.P. Wu, H.Q. Wu, Electrochem. Commun. 8 (2006) 1553–1557.
[13] C. Pouillerie, L. Croguennec, Ph. Biensan, P. Willmann, C. Delmas, J. Electrochem. Soc. 147 (2000) 2061–2069.
[14] C. Pouillerie, F. Perton, Ph. Biensan, J.P. Pérès, M. Broussely, C. Delmas, J. Power Sources 96 (2001) 293–302.